Available online at www.sciencedirect.com
SCIENCE DIRECT®
International Journal of Pharmaceutics 264 (2003) 15–24
international journal of pharmaceutics
www.elsevier.com/locate/ijpharm

Stabilization of DNA utilizing divalent cations and alcohol

Jefferson D. Knight[1], Roger C. Adami*

Department of Pharmaceutical Research and Development, Pfizer Global Research and Development, Groton Laboratories, MS 8156-26, Groton, CT 06340, USA

Received 10 April 2003; received in revised form 24 June 2003; accepted 1 July 2003

Abstract

A novel method for protection of DNA from high shear induced damage is presented. This method uses simple divalent cations and the lyophilizable alcohol, *tert*-butanol, to self-assemble DNA into condensed, shear-resistant forms. The DNA used in these studies was a 5600 BP plasmid DNA encoding a therapeutic gene. Various solvents and salts were used to identify optimal conditions to condense plasmid DNA. A stable formulation was identified with plasmid DNA condensed in a cosolvent solution containing 20% (v/v) *tert*-butanol and 1 mM calcium chloride. The DNA was formulated at 100 μg/ml and condensed into rod and toroidal shapes that were approximately 50–300 nm in diameter. The rods were found to be kinetically stable for greater than 24 h following their preparation. Condensation of the plasmid DNA in this manner results in nearly 100% of the plasmid DNA remaining intact after 1 min of high shear stress applied by a 50 W probe sonicator. Uncondensed control plasmid DNA is completely fragmented following 30 s of identical sonication. It is believed that condensation of DNA in this manner will permit utilization of high shear-stress inducing processing techniques, such as lyophilization or spray-drying without resulting in damage to the DNA.

Keywords: Stabilization; DNA; Solvent; Gene therapy; Ion-pair complex

1. Introduction

The utilization of naked DNA as a pharmaceutical product requires adequate stability of the formulation during both the manufacturing process and upon long-term storage. DNA is a labile molecule that is susceptible not only to chemical degradation via hydrolytic (Waterman et al., 2002a) and oxidative pathways (Waterman et al., 2002b), but is also sensitive to damage induced by shear (Adami and Rice, 1999; Lengsfeld and Anchordoquy, 2002). Processing of DNA during manufacture of the drug product can result in many medium and high shear processes that affect the stability of the DNA. Examples of such medium to high shear processes are mixing, turbulent flow during transport, filtration, lyophilization, and spray-drying. Since any strand breakage that occurs in the DNA affects the quality and performance of the drug product, especially if the damage is in the promoter or gene-coding region, it is imperative to address the potential of shear related damage that may occur during processing of the DNA (Lengsfeld and Anchordoquy, 2002).

Protecting DNA from damage is of paramount importance in biological systems. The natural self-assembling attributes of DNA permit structural

* Corresponding author. Tel.: +1-860-715-4204; fax: +1-860-441-0467.
E-mail address: adamirc@groton.pfizer.com (R.C. Adami).
[1] Present address: Department of Pharmacology, Yale University, New Haven, CT 06520, USA.

0378-5173/$ – see front matter © 2003 Elsevier B.V. All rights reserved.
doi:10.1016/S0378-5173(03)00367-3

rearrangement by physical manipulation with materials that bind and condense the DNA. In nature, condensation and tight packaging of chromosomal DNA, with histones in the cell nucleus, has evolved to not only reduce the size of the DNA but also to stabilize the DNA. Although organisms have elaborate mechanisms for packaging their DNA, a similar collapse of extended DNA into compact structures has been observed in vitro through the addition of various complexation agents (Manning, 1978; Wilson and Bloomfield, 1979; Widom and Baldwin, 1980).

Many of the condensation reagents, including cationic lipids (Wheeler et al., 1996), peptides (Adami et al., 1998), and cationic polymers (Ogris et al., 1998; Tang and Szoka, 1997), have been studied as transfection agents in nonviral gene therapy. These excipients typically ion-pair with the anionic phosphate backbone of DNA resulting in the condensation of the DNA, which provides a compact and stabilized form for gene delivery. Additionally, it has been shown that the polycationic condensing agents protect DNA from nucleolytic enzyme and sonication-induced degradation (Adami and Rice, 1999). Despite their many advantages, however, high molecular weight condensing agents are not without their drawbacks and have met with limited success in vivo due to their cytotoxicity (Wolfert et al., 1996) and complement activation (Plank et al., 1996).

Naked DNA gene therapy clinical trials represent approximately 10% of the protocols currently being conducted (Journal of Gene Medicine, "Protocols by Vector" online at http://www.wiley.co.uk/genetherapy/clinical/ on 24 June 2002). Naked DNA is typically plasmid DNA formulated in a buffer that protects the DNA from chemical degradation, but does not include excipients to complex the DNA and protect it from physical degradation. Additionally, it is sometimes lyophilized to extend room-temperature stability, although there is data suggesting that lyophilization may damage the DNA leading to a loss of transfection efficiency (Poxon and Hughes, 2000). Although the formulation is simple, manufacturing the final drug product requires stabilizing the highly labile naked DNA to process-induced shear stresses.

We sought to use a lyophilizable alcohol and simple dications to achieve DNA stabilization. Condensation of DNA by polycationic proteins was first proposed by McGhee and von Hippel (1974). Application of these condensation theories to inorganic polycations was conducted by Manning (1978) and experimentally demonstrated by Wilson and Bloomfield (1979). The two major forces driving cation-induced condensation are a reduction in repulsion between DNA segments and an increased attractive force based on the fluctuations of correlated counterions (Marquet and Houssier, 1991). Structural manipulation of the DNA was achieved via solvent and cation selection. This study tested a hypothesis that condensation of DNA via solvents, particularly the lyophilizable alcohol *tert*-butanol (Kasraian and DeLuca, 1995), and simple cations would result in condensed stabilized forms of DNA.

2. Materials and methods

2.1. Materials

A proprietary therapeutic 5600 BP plasmid DNA encoding feline erythropoietin (80% supercoiled, 18% open circular) was used in the experiments below. Construction, sequence and expression of the plasmid is described in European Patent Application 99 309201.4, published on 28 June 2000 as EP 1 013 288 A2. The salts zinc chloride, magnesium chloride hexahydrate, were from Aldrich, and the calcium chloride was from Fisher. The alcohols used were methanol (J.T. Baker), 2-methyl-2-propanol (*tert*-butanol, *t*-BuOH) (Aldrich), and ethanol (Pharmco). All dilutions were into water purified via the Alpha-Q water purification system (Millipore). Stocks of DNA, alcohol, salt, and water were prepared and filtered through a Millex-GP 0.22 μm filter unit prior to use.

2.2. Preparation of condensed naked DNA formulations

A deionized solution of plasmid DNA (5600 BP) was prepared by washing the DNA on a 10,000 MWCO Amicon ultra-dialysis membrane using 10 volumes of deionized water. The deionized DNA was dissolved in diH_2O to a 1 mg/ml stock solution. The DNA was diluted to the desired concentration in an

aqueous alcohol solution. The alcohols used were methanol, ethanol, isopropanol, and *tert*-butanol. Various amounts of the chloride salt form of zinc, magnesium, or calcium were added to the alcohol/DNA solution. The solutions were mixed well by vortexing and incubated for 1–1.5 h at room temperature.

2.3. Design of experiment

A central composite experimental design was implemented to determine the optimal conditions to identify a phase space for condensation of the plasmid DNA. The central composite design incorporated five factors. Three factors were internal: plasmid concentration, ion concentration, and pH, and two were external factors: temperature, and time. The central composite design had 8 cube points, 2 center points, and 6 star points. The order the experiments were performed was randomized. The cube points consisted of the full factorial design points, allowing assessment of both main effects as well as possible interactions among the three internal factors. Six axial points were added to provide information on possible nonlinear effects. The positions were chosen to ensure rotatability of the design, which ensured that for a given distance from the center of the design, the variability of the predictions was the same in all directions.

2.4. Determination of DNA condensation

Condensed DNA was distinguished from uncondensed DNA by centrifugation and absorbance measurement. Samples were centrifuged for 4 min at 15,800 × *g*. An 80-μl aliquot from the top of the supernatant was diluted 1:10 and concentration of DNA was measured (A_{260} nm) and compared to that of a corresponding aliquot taken prior to centrifugation. The difference in absorbance was correlated to the amount of DNA remaining in suspension. Uncondensed forms of DNA would remain buoyant and have similar absorbance values before and after centrifugation. Aggregates and condensed particles would settle and absorbance would be lower following centrifugation. Alternatively, for sample DNA concentrations $\leq$50 μg/ml, the aliquots were diluted into 1× GelStar DNA stain (FMC BioProducts) and analyzed on a Hitachi F-2000 fluorescence spectrophotometer (excitation 493 nm, emission 527 nm) with similar results.

2.5. Particle size measurements

Particle size measurements were performed on a 90Plus Particle Size Analyzer from Brookhaven Instruments Corporation (Holtsville, NY). Three runs of 1 min each were performed for each sample, and the mean of the three runs was reported. Solvent viscosity of a 20% *t*-BuOH solution was 1.723 cP as measured on a TA Instruments AR1000 rheometer and this viscosity value was used in the measurement of particle size in the dynamic light scattering mode. The particle size measurements accounted for the intrinsic light scatter of 20% *t*-BuOH in water, which resulted in reported particle sizes similar to those of condensed DNA (Finney et al., 2000). The DNA particles were distinguished from this background by the count rate. DNA samples were considered uncondensed if the light scattering count rate was not at least two times higher than the same sample without DNA and at least two times higher than the same sample without $CaCl_2$. Samples with a count rate less than three times higher than the control were investigated further via centrifugation and absorbance to determine if condensation was present.

2.6. Electron microscopy

Samples were prepared and incubated at room temperature for 1.5 h before being stained for electron microscopy. Formvar coated copper grids (200 mesh) were treated by glow discharge for 2 min. A drop of the DNA was floated on the grid for 60 s and blotted dry. A 2% uranyl acetate stain was then applied for 60 s and blotted dry. Grids were viewed on a Hitachi electron microscope at 50,000× magnification at 100 kV power.

2.7. Light scattering studies

The kinetics of particle formation were investigated with a Hitachi F-2000 fluorescence spectrometer with excitation and emission wavelengths set to 400 nm. The total light scattered at 90° of an equilibrated solution of DNA in *t*-BuOH was measured for a 5 s interval. Increase in light scattered was measured as a

function of time after the addition and thorough mixing of $CaCl_2$ to the DNA/*t*-BuOH solution.

2.8. Measurement of zeta potential

The zeta potential of DNA condensed with 20% *t*-BuOH and 1 mM $CaCl_2$ was measured using a 90Plus Particle Size Analyzer from Brookhaven Instruments Corporation. Zeta potential was calculated using the Smoluchowski model with the viscosity set at 1.723 cP and the dielectric constant as 66.5. Six runs of 15 cycles each were performed and the average zeta measurement was reported.

2.9. Shear-stress resistance

Samples were prepared as described above and incubated for 24 h at room temperature. One milliliter aliquots of condensed DNA formulations and uncondensed controls were sonicated for various amounts of time using a Cole Parmer 4710 Series 50 W probe sonicator. Damage to the DNA was analyzed by electrophoresis through a 1.1% Seakem agarose gel (FMC BioProducts) electrophoresed for 60 min at 80 V and stained using Sybr®-Gold (Molecular Probes, Eugene, OR). A linear DNA marker was obtained by restriction digest of the plasmid DNA with EcoRV (Gibco). Quantitative densitometry was performed by scanning the gel on a Molecular Dynamics™ Fluorimager (Amersham Biosciences, Piscataway, NJ) and using ImageQuant software to calculate relative band intensities.

3. Results

Conditions that led to DNA condensation were rapidly screened using a centrifugation assay that measured the sedimentation of condensed DNA. Condensation of plasmid DNA at 100 μg/ml in various concentrations of $MgCl_2$, $CaCl_2$, and $ZnCl_2$ and methanol, ethanol, or *t*-BuOH was investigated (Table 1). Depending on the conditions, the structure of the plasmid DNA resulted in either (1) uncondensed DNA, (2) precipitated aggregates, or (3) structured condensed particles. Both the aggregates and the condensed form led to a 5–10-fold decrease in absorbance after centrifugation, while uncondensed DNA had a reduction of 15% or less. In all solvents, except *t*-BuOH, aggregation, which was manifested as formation of visible flocculates, occurred most rapidly with $MgCl_2$. However, the magnesium salt was the least effective of the three salts for condensing DNA in *t*-BuOH solutions, requiring a higher concentration to induce condensation. In 80% (v/v) *t*-BuOH, precipitation occurred overnight in the presence of any ion. A central composite factorial design experimental methodology was used to determine the optimal conditions that lead to condensation within the vicinity of the initially identified region (data not shown). Conditions that led to robust DNA condensation occurred at 100 μg/ml plasmid DNA in 20% *t*-BuOH with 1 mM $CaCl_2$.

Optimization of conditions leading to condensation without aggregation in 20% *t*-BuOH and 1 mM $CaCl_2$ was performed by varying solution conditions around this point (Fig. 1). Condensation without

Table 1
Initial salt–alcohol condensation screening assay

Salt	Methanol (50%)	Ethanol (50%)	*t*-BuOH (20%)	*t*-BuOH (50%)	*t*-BuOH (80%)
0.1 mM $CaCl_2$	–	–	–	–	24
1 mM $CaCl_2$	4	3	Condensed	24	24
10 mM $CaCl_2$	1.5	3	3	24	1
0.1 mM $ZnCl_2$	–	–	–	–	24
1 mM $ZnCl_2$	3	3	–	24	24
10 mM $ZnCl_2$	4	3	3	24	24
0.1 mM $MgCl_2$	–	–	–	–	24
1 mM $MgCl_2$	3	3	–	–	24
10 mM $MgCl_2$	1	1	3	2	1

Samples were observed following the addition of the indicated amount of salt to solvent containing 100 μg/ml plasmid DNA. Numbers indicate time (h) when visible aggregation was first noticed; (–) indicates samples which did not show a decrease in absorbance after centrifugation. Sample that was condensed but did not visibly aggregate is marked “condensed.”

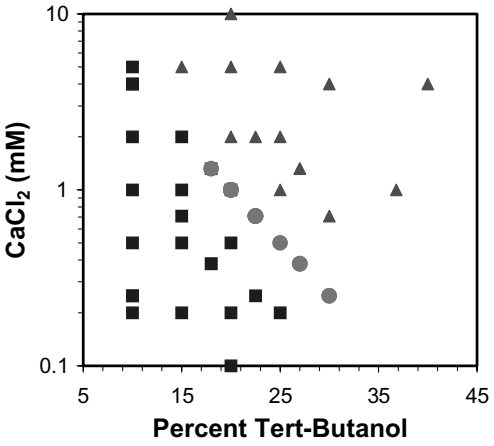

Fig. 1. Conditions for condensation of DNA in *t*-BuOH and $CaCl_2$. Condensation was determined by centrifugation and absorbance and/or by count rate comparison of particle size measurements. Circles (●) indicate conditions leading to condensation, squares (■) indicate lack of condensation, and triangles (▲) indicate formation of visible flocculates. Conditions selected to perform the condensation for further experiments were 20% *t*-BuOH and 1 mM $CaCl_2$.

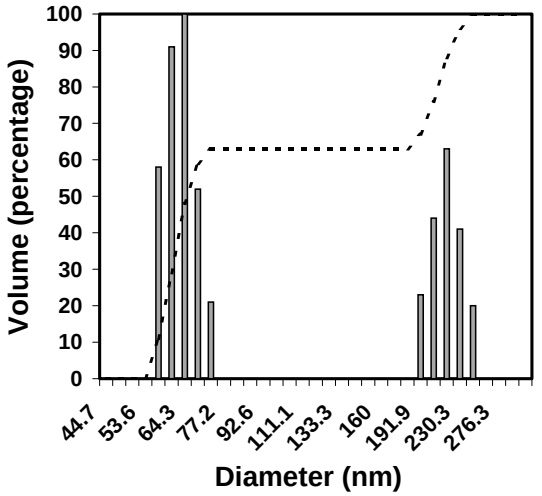

Fig. 2. Calcium chloride induced condensation leads to compaction of the DNA which can be quantified using quasielastic light scattering particle sizing. There is a bimodal distribution of particle sizes due to differences in the hydrodynamic radii of the smaller diameter toroids and larger diameter rods following $CaCl_2$ condensation. In this representative sample 63% of the particles (by volume) have a diameter centered at 64 nm and 37% of the particles have a diameter centered at 220 nm.

aggregation was found in a narrow range of conditions, with less $CaCl_2$ required as the *t*-BuOH concentration increased. The effect of varying the DNA concentration was also investigated, and it was found that more $CaCl_2$ was required for condensation as the DNA concentration was increased, although this dependence was much less dramatic than that of the salt-alcohol concentrations.

Particle size data for DNA condensed with 20% *t*-BuOH and 1 mM $CaCl_2$ indicated that two populations of particles spontaneously formed in solution. The diameters of the two populations of particles were 40–70 and 200–500 nm (Fig. 2). These sizes correspond to two forms seen with electron microscopy: a toroid form with diameter 50–100 nm and a rod-like form that is approximately 25–50 nm in width and several hundred nm in length (Fig. 3B).

The kinetics of particle formation was investigated using total intensity light scattering at 400 nm (Fig. 4). The results show two phases of particle formation: the first, seen also in the control, occurs within 2 min after the addition of $CaCl_2$ and is thought to reflect a structural arrangement of the solvent system upon the addition of salt. After 5 min, the light scattering intensity was dominated by condensed DNA, which reached a plateau after 1 h and remained there for several hours. Visible aggregation of these particles was not noticed after 24 h, although the fraction of particles in the 200–500 nm size range was greater (data not shown).

The effect of temperature on particle formation relative to background was studied using particle size measurements (Fig. 5). As shown in Fig. 5A, the count rate increased with increasing temperature while the background count rate decreased with increasing temperature. The reported particle size decreased for both sample and control with increasing temperature, although the decrease between 30 and 70 °C was greater for the control (55%) than the DNA-containing sample (40%) (Fig. 5B).

The zeta potential of DNA particles condensed with 20% *t*-BuOH and 1 mM $CaCl_2$ was determined to be -17.28 ± 1.29 mV under an electric field of 7.24 V/cm.

The shear-stress stability of DNA condensed with 20% *t*-BuOH and 1 mM $CaCl_2$ was investigated using a probe sonicator to induce shear stress. The structure of DNA condensed with 20% *t*-BuOH and 1 mM

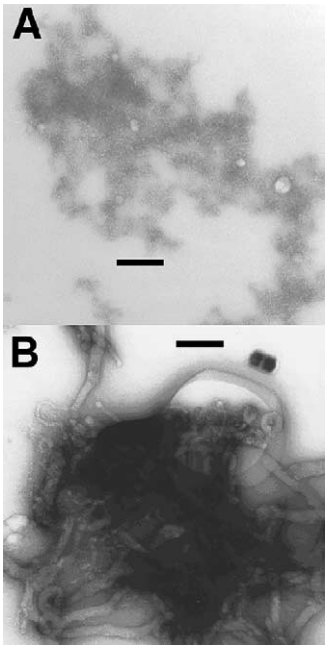

Fig. 3. Transmission electron microscope photos of DNA in 20% *t*-BuOH with 1 mM $CaCl_2$ (panel B) and without 1 mM $CaCl_2$ (panel A). The magnification of both photos is 50,000× and the scale bar length is 270 nm. Panel B shows the presence of rods and toroids (~100 nm diameter) of DNA following condensation with 1 mM $CaCl_2$.

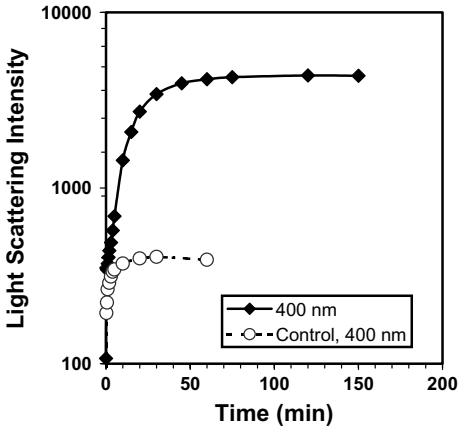

Fig. 4. Kinetics of particle formation. Condensation of DNA was monitored using light scatter at 400 nm. Scatter intensity reaches a plateau 45 min after the addition of $CaCl_2$, indicating completion of condensation. The control sample of 20% *t*-BuOH demonstrates a scatter intensity less than 10% that of the condensed particle.

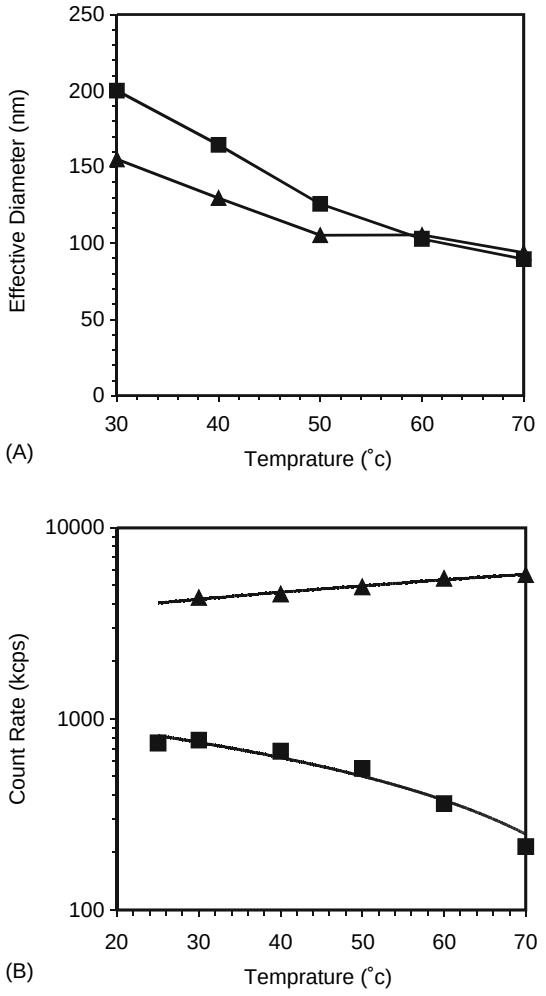

Fig. 5. Temperature dependence of particle size and light scatter in active (▲) vs. control (■) sample. Panel A represents the decreasing particle size formed at higher temperatures, decreasing from 155 nm at 30 °C to 95 nm at 70 °C. Panel B demonstrates the inverse relationship between the increasing count-rate of scattered light from condensed DNA at higher temperatures vs. decreasing counts for the control.

$CaCl_2$ was protected from the sonication-induced shear-stress damage, Fig. 6. The numbers above the lanes indicate time (s) of exposure to 50 W probe sonication. Following 30 s of sonication nearly 100% of the uncondensed open circular, linear, and supercoiled forms of the plasmid DNA are degraded resulting in the fragment smear seen at the bottom of the gel. In contrast, the condensed DNA retains 100% of the supercoiled and open circular form of the plasmid

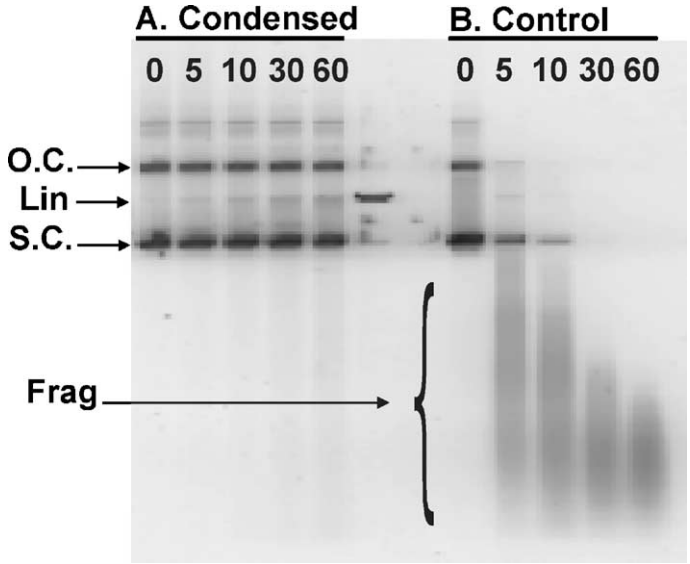

Fig. 6. Shear protection of DNA in condensed (A) and uncondensed (B) form. Numbers above the lanes indicate time (s) of exposure to 50 W probe sonication. Following 30 s of sonication 100% of the uncondensed open circular, linear, and supercoiled forms of the plasmid DNA are completely degraded resulting in the fragment smear seen at the bottom of the gel. In contrast, the condensed DNA retains 100% of the supercoiled and open circular form of the plasmid DNA following 60 s of sonication.

DNA following 60 s of sonication. Fig. 7 shows the cavitation induced shear-stress protection afforded to condensed plasmid DNA. The total percent of intact DNA, defined as supercoiled, open circular, and linear forms of plasmid DNA, was 100% for the condensed DNA after 60 s of probe sonication (50 W). There was only a 3% loss of supercoiled DNA after 60 s. It is seen that more than 60% of the uncondensed DNA is degraded after only 5 s of sonication, and only 1.6% of the intact plasmid DNA remains after 60 s.

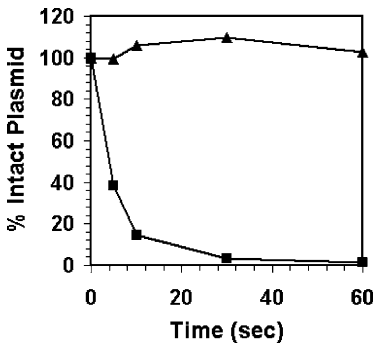

Fig. 7. Cavitation induced shear-stress protection afforded to condensed plasmid DNA exposed to 50 W probe sonication is shown. Triangles (▲) represent percent intact DNA remaining for condensed DNA after various exposure times. The percent of intact DNA is defined as supercoiled, open circular, and linear forms of plasmid DNA. Squares (■) represent the uncondensed control plasmid DNA. Only 1.6% of the intact plasmid DNA remains after 60 s.

While uncondensed DNA is degraded into oligonucleotide fragments after as little as 5 s of sonication, the majority of the condensed DNA was still in its initial supercoiled and open circular forms after 60 s of sonication.

4. Discussion

The condensation of DNA by inorganic polycations was first proposed by Manning (1978) and demonstrated by Wilson and Bloomfield (1979). The two major forces driving this cation-induced condensation are a reduction in repulsion between DNA segments and an increased attractive force based on the fluctuations of correlated counterions (Marquet and Houssier, 1991). DNA can be described as a polyanion with an average charge spacing of 1.7 Å, and the fraction of its charge r that is neutralized by N-valent cations present in solution is given by $r = 1 - (N\xi)^{-1}$. Here, ξ is a

dimensionless parameter determined by the solution conditions. In a solution of dielectric ε at temperature T, ξ is described by $\xi = q^2/\varepsilon kTb$, where q is the proton charge, k is Boltzmann's constant, and b is the linear charge spacing of the DNA (Manning, 1978; Wilson and Bloomfield, 1979). In water, the value of ξ for B-DNA is 4.2, and experimental results have shown that DNA condenses at $r \geq 0.90$, which can be achieved in water with a counterion of valence $N \geq 3$ (Wilson and Bloomfield, 1979). In a less polar solvent, divalent cations are sufficient, and ethanol alone can promote condensation into orderly, compact particles when the conditions are carefully controlled (Girod et al., 1973). Although DNA condensation by trivalent cobalt compounds has been extensively studied, considerably less is known about condensation with divalent metals in alcohol (Deng and Bloomfield, 1999; Ma and Bloomfield, 1994; Kejnovsky and Kypr, 1998). Condensation has been observed with Mg^{2+} in 50% methanol (Wilson and Bloomfield, 1979), and with trivalent metals in ethanol and isopropanol (Arscott et al., 1995), but to our knowledge has not been studied in binary aqueous solutions of *t*-BuOH.

tert-Butanol is the most nonpolar alcohol that is fully miscible with water (Bowron et al., 1998). The dielectric constant of 20% *t*-BuOH is 65, which corresponds to $r = 0.90$ for B-DNA and a divalent cation. Another interesting physical property of *t*-BuOH is that it has a much higher freezing point than ethanol and can be used in lyophilization (Finney et al., 2000; Kasraian and DeLuca, 1995). Given these properties, pharmaceutical preparations of plasmid DNA should be able to be condensed with divalent cations in 20% *t*-BuOH and subsequently manipulated via different processes, such as lyophilization or spray-drying to enhance long-term plasmid stability.

According to Manning's (1978) theory, any divalent cation should be able to condense DNA under these conditions, provided its concentration is sufficiently higher than that of residual monovalent counterions present with the DNA. However, at 1 mM salt in *t*-BuOH we only observe condensation with Ca^{2+}, and not with Mg^{2+} or Zn^{2+} (Fig. 1). The specificity for condensation in the presence of one species over another of the same valence is based on coulombic interactions. Rouzina and Bloomfield (1996) have shown that, due to an electrostatic mechanism, a smaller ion can fit better into DNA grooves to induce bending and condensation. Although Ca^{2+} has the largest ionic radius of the three in crystal form, it has the smallest hydrodynamic radius in aqueous solution, and thus the highest charge to surface area of the three divalent ions studied (Paulsen et al., 1988).

We show that DNA condensation occurs reproducibly in 20% *t*-BuOH with 1 mM Ca^{2+} and 100 μg/ml DNA. This corresponds to a molar ratio of 3:1 Ca^{2+}:DNA phosphate. The range of conditions under which we observe condensation is very narrow compared with those observed with trivalent cations in aqueous solution, suggesting that our condensates may be a thermodynamically metastable self-assembled form, which kinetically proceeds slowly on a pathway toward a lower energy aggregate. The rodlike forms we observe are often found when DNA is condensed in a solvent with low dielectric (Arscott et al., 1995), and may be more susceptible to eventual aggregation than toroids. Our condensates reached an equilibrium particle size in 1–2 h (Fig. 4) and did not aggregate within several days, which is an appropriate timescale for pharmaceutical processing.

The lifetime of the condensed form and the ratio of rod to toroid condensation could be further improved by optimization of several parameters, including temperature. We observe a general decrease in effective diameter with increasing temperature, indicating a shift to smaller, aggregation-resistant particles (Fig. 5A). The decreased effective diameter does not represent a transition to the uncondensed state, as the count rate did not decrease with increasing temperature (Fig. 5B). We suggest that larger particles may disassemble into smaller condensed particles at a transition temperature lower than that of smaller particles unraveling.

The condensed DNA particles we observe have a negative surface charge due to the fact that divalent cations in this solvent system are not expected to fully neutralize the negative charge of the DNA. This negative charge is in stark contrast to DNA condensed with liposomes or lysine-rich peptides, which are positively charged. The negatively charged surface permits further complexation with cationic species to further modify the properties of the DNA, or develop enhanced formulations.

The property of the condensed DNA that was most interesting and unexpected was the remarkable degree of stability imparted to the DNA following condensation (Fig. 6). Essentially 100% of the condensed

DNA remained intact following sonication. In contrast, 100% of the uncondensed control DNA was degraded under identical shear conditions (Fig. 7). The degree of stabilization maintained following sonication was equivalent to the amount of stabilization provided in peptide condensed DNA formulations (Adami et al., 1998). This finding suggests that collapsing the DNA upon itself into a rigid and condensed structure is all that is required to fully stabilize the DNA from shear-induced strand breakage.

We conclude that this method of stabilizing DNA is highly effective for use in a variety of process operations, such as spray-drying, filtration, mixing, or lyophilization. Additionally, it may be possible to further modify the condensed structures by applying formulation molecules, such as peptides, polymers, cationic lipids, and other cationic formulation molecules to the surface of the DNA condensates. This approach to stabilizing DNA results in an effective and safe way to process DNA.

Acknowledgements

The authors would like to acknowledge David Potter for assistance in the experimental design, Hans Stukenbrok for preparing EM grids and Germaine Boucher for performing the electron microscopy, Niomi Peckham for performing the densitometry calculations, and Kasra Kasraian and Ken Waterman for constructive feedback on the paper.

References

Adami, R.C., Rice, K.G., 1999. Metabolic stability of glutaraldehyde cross-linked peptide DNA condensates. J. Pharm. Sci. 88, 739–746.

Adami, R.C., Collard, W.T., Gupta, S.A., Kwok, K.Y., Bonadio, J., Rice, K.G., 1998. Stability of peptide-condensed plasmid DNA formulations. J. Pharm. Sci. 87, 678–683.

Arscott, P.G., Ma, C., Wenner, J., Bloomfield, V.A., 1995. DNA condensation in alcohol-water mixtures: dielectric constant and other solvent effects. Biopolymers 36, 345–365.

Bowron, D.T., Finney, J.L., Soper, A.K., 1998. Structural investigation of solute-solute interactions in aqueous solutions of tertiary butanol. J. Phys. Chem. B 102, 3551–3563.

Deng, H., Bloomfield, V.A., 1999. Structural effects of cobalt-amine compounds on DNA condensation. Biophys. J. 77, 1556–1561.

Finney, J.L., Bowron, D.T., Soper, A.K., 2000. The structure of aqueous solutions of tertiary butanol. J. Phys. Condens. Matter 12, A123–A128.

Girod, J.C., Johnson Jr., W.C., Huntington, S.K., Maestre, M.F., 1973. Conformation of deoxyribonucleic acid in alcohol solutions. Biochemistry 12, 5092–5097.

Kasraian, K., DeLuca, P.P., 1995. Thermal analysis of the tertiary butyl alcohol-water system and its implications on freeze-drying. Pharm. Res. 12, 484–490.

Kejnovsky, E., Kypr, J., 1998. Millimolar concentrations of zinc and other metal cations cause sedimentation of DNA. Nucleic Acids Res. 26, 5295–5299.

Lengsfeld, C.S., Anchordoquy, T.J., 2002. Shear-induced degradation of plasmid DNA. J. Pharm. Sci. 91, 1581–1589.

Ma, C., Bloomfield, V.A., 1994. Condensation of supercoiled DNA induced by $MnCl_2$. Biophys. J. 67, 1678–1681.

Manning, G.S., 1978. The molecular theory of polyelectrolyte solutions with applications to the electrostatic properties of polynucleotides. Q. Rev. Biophys. 11, 178–246.

Marquet, R., Houssier, C., 1991. Thermodynamics of cation-induced DNA condensation. J. Biomol. Struct. Dyn. 9, 159–167.

McGhee, J.D., von Hippel, P.H., 1974. Theoretical aspects of DNA-protein interactions: co-operative and non-co-operative binding of large ligands to a one-dimensional homogeneous lattice. J. Mol. Biol. 86, 469–489.

Ogris, M., Steinlein, P., Kursa, M., Mechtler, K., Kircheis, R., Wagner, E., 1998. The size of DNA/transferrin-PEI complexes is an important factor for gene expression in cultured cells. Gene Ther. 5, 1425–1433.

Paulsen, M.D., Anderson, C.F., Record Jr., M.T., 1988. Counterion exchange reactions on DNA: Monte Carlo and Poisson-Boltzmann analysis. Biopolymers. 27, 1249–1265.

Plank, C., Mechtler, K., Szoka Jr., F.C., Wagner, E., 1996. Activation of the complement system by synthetic DNA complexes: a potential barrier for intravenous gene delivery. Hum. Gene Ther. 7, 1437–1446.

Poxon, S.W., Hughes, J.A., 2000. The effect of lyophilization on plasmid DNA activity. Pharm. Dev. Tech. 5, 115–122.

Rouzina, I., Bloomfield, V.A., 1996. Influence of ligand spatial organization on competitive electrostatic binding to DNA. J. Phys. Chem. 100, 4305–4313.

Tang, M.X., Szoka, F.C., 1997. The influence of polymer structure on the interactions of cationic polymers with DNA and morphology of the resulting complexes. Gene Ther. 4, 823–832.

Waterman, K.C., Adami, R.C., Alsante, K.M., Antipas, A.S., Arenson, D.R., Carrier, R., Hong, J., Landis, M.S., Lombardo, F., Shah, J.C., Shalaev, E., Smith, S.W., Wang, H., 2002a. Hydrolysis in pharmaceutical formulations. Pharm. Dev. Tech. 7, 113–146.

Waterman, K.C., Adami, R.C., Alsante, K.M., Hong, J., Landis, M.S., Lombardo, F., Roberts, C.J., 2002b. Stabilization of pharmaceuticals to oxidative degradation. Pharm. Dev. Tech. 7, 1–32.

Wheeler, C.J., Felgner, P.L., Tsai, Y.J., Marshall, J., Sukhu, L., Doh, S.G., Hartikka, J., Nietupski, J., Manthorpe, M., Nichols, M., Plewe, M., Liang, X., Norman, J., Smith, A., Cheng, S.H., 1996. A novel cationic lipid greatly enhances plasmid DNA delivery and expression in mouse lung. Proc. Natl. Acad. Sci. U.S.A. 93, 11454–11459.

Widom, J., Baldwin, R.L., 1980. Cation-induced toroidal condensation of DNA: studies with $Co^{3+}(NH_3)_6$. J. Mol. Biol. 144, 431–453.

Wilson, R.W., Bloomfield, V.A., 1979. Counterion-induced condensation of deoxyribonucleic acid. A light-scattering study. Biochem. 18, 2192–2196.

Wolfert, M.A., Schact, E.H., Toncheva, V., Ulbrich, K., Nazarova, O., Seymour, L.W., 1996. Characterization of vectors for gene therapy formed by self-assembly of DNA with synthetic block co-polymers. Hum. Gene Ther. 7, 2123–2133.